Studies on a new low carbon amorphous binder

Álvaro José Lebres Mendes
alvaro.lebres.mendes@tecnico.ulisboa.pt

Instituto Superior Técnico, Av. Rovisco Pais, 1049-001 Lisboa, Portugal

ABSTRACT

This work studies the effects that fineness, the mill used in grinding and storage time after grinding have on the binder's reactivity, and also presents a study on the optimization of the minimum amount of sodium silicate necessary in the alkaline activation of the new amorphous hydraulic binder to obtain competitive mechanical performances to that of OPC, as well as the possible replacement of sodium silicate with alternative activators such as sodium sulphate and calcium sulphate to reduce the alkaline activation costs. This work also provides a study on the optimization of the water/cement ratio in alkali-activated mortars, in order to obtain better compressive strengths and a workability equivalent to a standard cement. It was concluded that fineness has a strong influence on the initial reactivity of the amorphous, nonetheless, with a fineness similar to that of the OPC it is still possible to achieve competitive compressive strengths. In addition, it was found that the type of mill used and the storage time after milling do not significantly influence the reactivity of the amorphous. The necessary amount of sodium silicate in the alkaline activation was optimized, reducing, at least, 25% of the previously used amount without negatively impacting the mechanical performance. It was found that the alkaline activation with sodium sulfate and calcium sulfate do not present competitive results and that the best workability and mechanical performances in mortar are achieved, respectively for a water/cement ratio of 0.38 and 0.365.

Keywords: Amorphous hydraulic binders, fineness, grinding, storage time, alkaline activators, water/cement ratio optimization

1. Introduction

The production of Portland cement (OPC) stands today close to 4 billion tons per year and it is expected to grow to 5 billion tons per year by 2050 [1]. Despite this growth represents a positive socioeconomic event, its potential impact on the climate change is an issue that deserves particular attention. Nowadays, the production of OPC clinker releases an estimated ~0.8 ton CO_2/ton clinker, representing 5-6% of total manmade greenhouse gases [2] [3] [4]. The major emissions of cement industries come from cement clinker production in the kiln system [5]. Hence with increasing building demands in the near future, the development of a hydraulic binder that reduces the ecological footprint without jeopardizing the technical, economic and workability characteristics of the OPC is a challenge of the upmost importance for the cement industry [3] [6] [7].

Over the last few years, a lot of effort has been put towards the development of eco-friendly alternatives to traditional OPC, such as the increase of clinker replacement in cement mixtures using, for example supplementary cementitious materials (SCM) like clays rich in metakaolin and limestone [8] and the development of new types of cements like belite-rich cements [9] and alkali-activated

cements [10], to reduce the amount of CO_2 emitted. Nevertheless, due to the lack of extensive availability in the desired qualities of the raw materials needed to produce these new cement types, these solutions are still far from representing a real alternative to OPC.

Thus, in an attempt to develop an alternative to OPC that addresses the CO_2 emissions problem and making use of most of the existing clinker production technology, Santos *et. al* [11], proposed a process consisting in fully melting and rapid cooling a mixture of conventional raw materials in cement manufacture, in such an amount that reduces in about 25% the process related CO_2 emissions when compared to the typical OPC process, producing a low calcium amorphous binder, with a CaO/SiO_2 molar ratio of 1.1. This new binder is hydraulically active and demonstrates promising compressive strengths of alkali-activated pastes with Na_2SiO_3 [12], revealing a fast development of compressive strength at early age reaching compressive strengths similar to those of OPC. Following these promising results in pastes, it was proven the need to further investigate this amorphous binder, starting with the study of its application in mortars and concrete.

This work studies the effects of fineness, the mill used in grinding and storage time on the reactivity of the aforementioned amorphous binder. It also presents optimization studies on the alkali-activation of pastes and on the W/C of mortar samples prepared with this new binder.

2. Materials and experimental techniques

In this work, a mixture of three different raw materials was prepared to produce a low calcium hydraulic binder, comprising limestone as a source of calcium, sand as a source of silica and a cement raw meal as a source of alumina and calcium. The chemical composition of each raw material and amorphous calcium silicate hydraulic binder was obtained via wavelength-dispersive X-ray fluorescence spectrometry, using an Axios cement from Malvern Panalytical and is displayed in Table 2, in section 7.

After mixing the raw materials, the raw meal was placed in a silicon carbide crucible and inserted in a furnace. The raw meal was subjected to fully melting, at 1550°C, and quenching in a water-cooling system. After quenching, the amorphous hydraulic binder was dried during 24 hours at 100°C, ground to a powder form in a ring mill or a ball mill, and, finally, stored in vacuum. Pastes were prepared by adding the ground binder to an aqueous alkaline solution acting as alkaline activator at a water/cement weight ratio (W/C) of 0.25, 0.263 or 0.27, in order to have a similar plasticity between all pastes in the each study. Mortars were prepared according to EN 196–1 [13], by mixing 450 g of the amorphous hydraulic binder with an aqueous alkaline solution of Na_2SiO_3 and NaOH at different W/C ratios, such as 0.38, 0.365, 0.35 and 0.335, and by adding 1350 g of AFNOR sand. Then, paste samples were poured into inox steel moulds with dimension of $20 \times 20 \times 40$ mm^3 while mortar samples were poured into inox steel moulds with dimension of $40 \times 40 \times 160$ mm^3 and cured at 20°C in a moisture-controlled environment with a relative humidity above 95%. The mechanical performance of each sample was studied using compressive strength tests, at 2, 7, 28 and 90 days, and the hydration evolution of pastes was followed by isothermal calorimetry and, thermogravimetric analysis (TGA).

All calorimetry experiments were performed with an isothermal calorimeter (TAM Air, Sweden) using glass ampoules, at 20°C and using water as a reference. The heat of hydration data was collected during 7 days.

The determination of the compressive strength of the pastes and mortars produced with the amorphous binder was done according to the EN 196–1 [13], using a cement strength testing machine, Autotest 400/10 (Ibertest, Spain) with a force rate of 2.4 kN/s.

The TGA measurements were performed to determine the amount of bound water in the C–S–H structure, assuming the loss of bound water between 105°C and 500°C, and were performed in an ELTRA multichannel TGA device (ELTRA, Germany) running at constant heating rates between fixed temperatures (105, 250, 500 and 950°C) maintained until a constant mass was reached. From room temperature to 105°C it was applied a heating rate of 4°C/min,

from 105°C to 250°C a heating rate of 10°C/min, from 250°C to 500°C and between 500°C and 950°C, the applied heating rate was 15°C/min.

To determine the workability of a mortar, the flow table test was performed, according to European standard EN 1015–3 [14].

Table 3 in section 7 shows the milling conditions and adopted nomenclature for each sample in the fineness, mill and storage time studies. It also shows the alkali-activation conditions and adopted nomenclature for each sample in the alkali-activation optimization studies.

3. Results

3.1. Fineness study

3.1.1. Isothermal calorimetry

Figure 1 shows the evolution of normalized heat flow and the normalized cumulative heat curves in function of time for each sample of binder B with greater fineness (*B_3min_Ring*) and lower fineness (*B_1min_Ring*), where it is possible to see that the greater the fineness, the sooner the peak of hydration is achieved and higher the amount of heat released after 7 days. *B_3min_Ring* reached the maximum of its hydration peak at ~ 9 hours, releasing 93,3 J/g of cumulative heat after 7 days, while *B_1min_Ring* reached the maximum heat flow at ~23 hours, releasing 77,1 J/g of cumulative heat after 7 days.

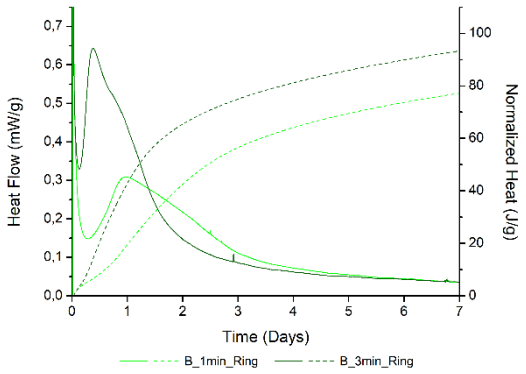

Figure 1 – Calorimetry results for paste samples with different fineness.

3.1.2. Compressive strength tests

The development of compressive strength over the time of hydration for paste samples with different fineness is displayed in Figure 2, demonstrating that samples with a higher fineness have the capacity to develop higher compressive strengths at early ages. At later ages, 28 and 90 days, that effect is practically negligible.

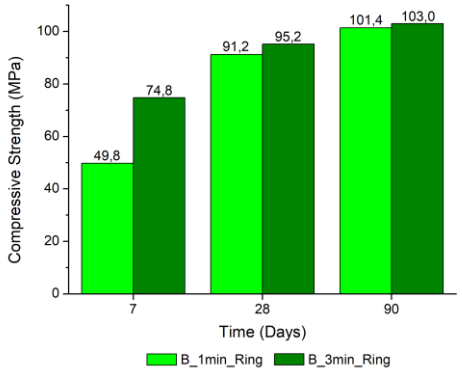

Figure 2 – Compressive strength results for paste samples with different fineness.

3.1.3. Thermogravimetric analysis

Figure 3 shows the evolution of the amount of bound water over time for the paste samples with different fineness. It can be verified that the sample *B_3min_Ring* presents higher amounts of bound water at all ages. Moreover, the rate of bound water development is almost parallel between the samples with different fineness, indicating that the difference in fineness does not have much influence in the development of bound water, and consequently C–S–H, through time, only in the amount of bound water at very early ages, giving them a huge boost in initial reactivity due to the greater number of nucleation sites. Nonetheless, it was expected that the amount of bound water of both samples would be closer at 28 and 90 days, considering the compressive strengths at these ages.

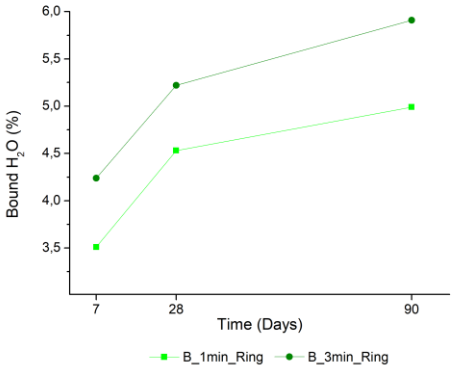

Figure 3 – TGA results for paste samples with different fineness.

3.2. Mill study

3.2.1. Compressive strength tests

Figure 4 illustrates the compressive strength results for the paste samples with similar fineness from different mills, revealing that both samples develop identical compressive strength, at 2 and 7 days of hydration. At 28 days, pastes differ by 11%, which is nearly within the acceptable error for this technique (10%) and can occur from possible minor defects in the paste samples and the test variability.

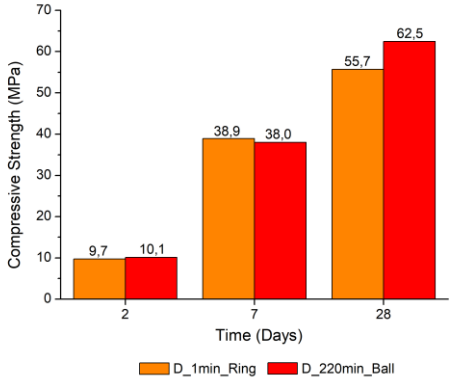

Figure 4 – Compressive strength results for paste samples with similar fineness.

3.2.2. Thermogravimetric analysis

Figure 5 shows the evolution of amount of bound water through time of hydration, where it is quite clear that the evolution of bound water of the sample ground in the ring mill (Blaine fineness value – 4054 cm^2/g) follows a very identical trend to the one ground in the ball mill (Blaine fineness value – 4351 cm^2/g) having almost equal amounts of bound water for all ages.

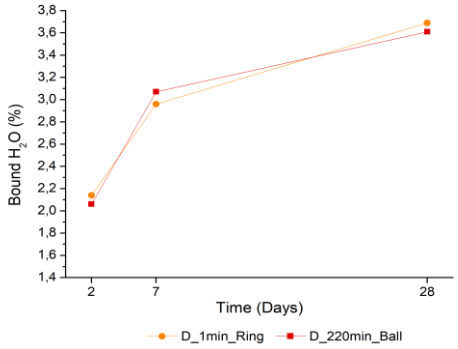

Figure 5 – TGA results for paste samples with similar fineness.

3.3. Storage time study

3.3.1. Isothermal calorimetry

The evolution of normalized heat flow and the normalized cumulative heat curves in function of time of hydration for samples with different storage times, 1 and 7 days respectively is displayed in Figure 6. Although the heat flow curve illustrates that *A_3min_Ring_7daysST* achieves the heat flow peak considerably later (~ 22 hours) than *A_3min_Ring_1dayST* (~ 9 hours), the total amount of heat released after 7 days is similar between the two samples, with sample *A_3min_Ring_7daysST* releasing 91,3 J/g while sample *A_3min_Ring_1dayST* released 85,4 J/g.

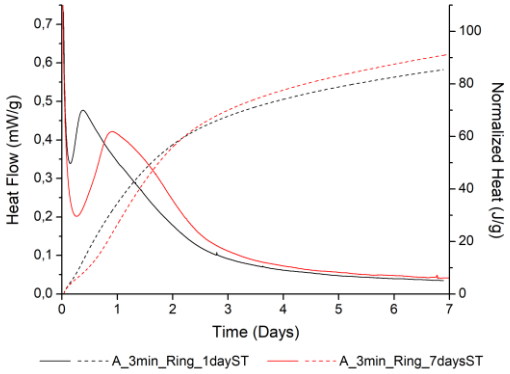

Figure 6 – Calorimetry results for paste samples with different storage times.

3.3.2. Compressive strength tests

Figure 7 displays the compressive strength results for samples of binder A with different storage time after milling and a sample of binder B with 1 day of storage time to have a reference point for the compressive strength as 90 days. The results show very similar compressive strengths at 7 days, validating the calorimetry results. At 28 days, *A_3min_Ring_7daysST* did not show a development in compressive strength, whereas *A_3min_Ring_1dayST* and *B_3min_Ring_1dayST* increased to 116,3 MPa and 95,2 MPa, respectively. This lack of improvement may be related to an imperfect test piece, that corrupted the real performance of the sample at 28 days.

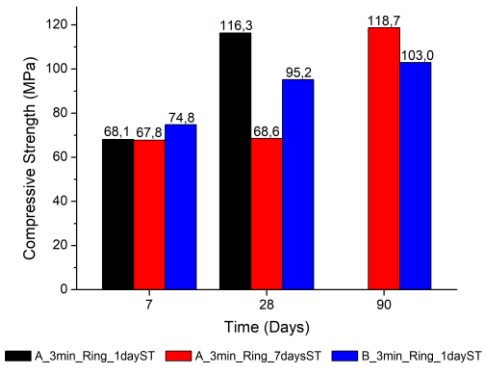

Figure 7 – Compressive strength results for paste samples with different storage times.

3.3.3. Thermogravimetric analysis

The amount of bound water for the paste samples with different storage time is displayed in Figure 8, showing that the sample with 7 days of storage time has an almost equal rate of bound water development over all ages as the other samples with only 1 day of storage time, indicating that reactivity across all three samples is very identical and that a storage time of up to 7 days does not affect the amount of hydration products formed significantly. Moreover, from 7 to 28 days, *A_3min_Ring_7daysST* exhibits a substantial increase in the amount of bound water, which should have translated into an increase in compressive strength at 28 days, which was not the case, confirming that the result of compressive strength at 28 days of this sample could be explained by a defective test sample.

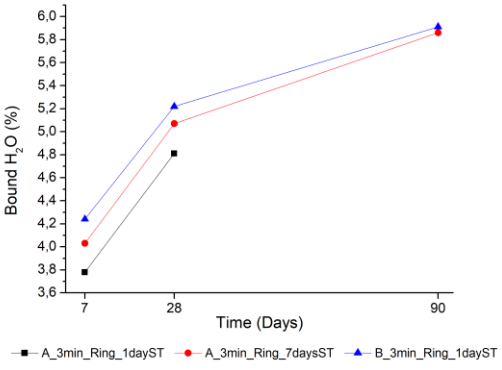

Figure 8 – TGA results for paste samples with different storage times.

3.4. Alkali-activation optimization studies

In this section, it is presented a study on the optimization of the minimum amount of sodium silicate (Na_2SiO_3) necessary in the alkaline activation of the amorphous binder to obtain competitive mechanical performances to that of OPC, as well as the possible replacement of Na_2SiO_3 with alternative activators such as sodium sulphate (Na_2SO_4) and calcium sulphate ($CaSO_4$) to reduce the alkaline activation costs and a study on the optimization of the water/cement ratio in alkali-activated mortars, in order to obtain better compressive strengths and a workability equivalent to a standard cement.

3.4.1. Na_2SiO_3 study

3.4.1.1. Isothermal calorimetry

In Figure 9, the evolution of normalized heat flow and the normalized cumulative heat curves in function of time of hydration for the samples with different amounts of Na_2SiO_3 in the alkaline activation solution is represented.

From the results, it is evident that the increase of Na_2SiO_3 successively delays the peak of hydration. However, after the peak, the reaction kinetics of samples with lower amounts of Na_2SiO_3 show a sudden significant drop, which is not seen in samples with higher Na_2SiO_3 content, namely 50%, 75% and 100% Na_2SiO_3, causing these samples to release more heat after 7 days, with the reference paste (100% Na_2SiO_3) releasing 62,2 J/g, whereas sample without Na_2SiO_3 only released 42,1 J/g.

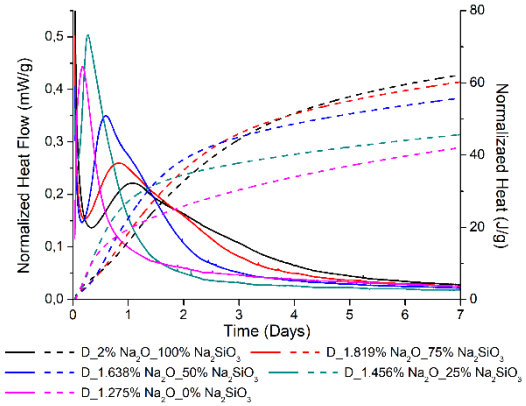

Figure 9 – Calorimetry results for paste samples with different amounts of Na_2SiO_3.

3.4.1.2. Compressive strength tests

Figure 10 shows the evolution of compressive strength from paste samples prepared with different amounts of Na_2SiO_3 in the alkaline activation solution. The results show that as the

amount of Na_2SiO_3 decreases, so does the compressive strength, except for very early ages, 2 days, where the best mechanical performance is achieved for the sample with 50% Na_2SiO_3, confirming the calorimetry results. Sample with 75% Na_2SiO_3 developed identical, or even better, mechanical performances than sample with 100% Na_2SiO_3, which is a promising result for the reduction of Na_2SiO_3 in the activation solution.

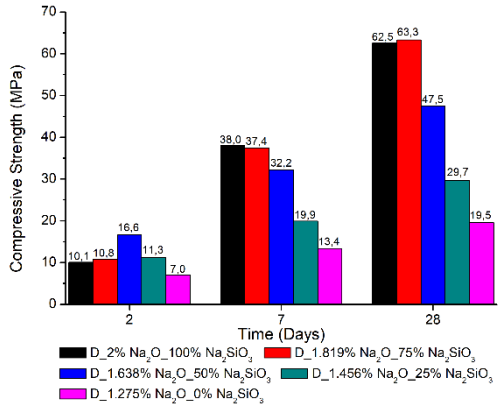

Figure 10 – Compressive strength results for paste samples with different amounts of Na_2SiO_3.

3.4.1.3. Thermogravimetric analysis

Figure 11 displays the development of the amount of bound water over the time of hydration for paste samples with different amounts of Na_2SiO_3, revealing that for larger amounts of Na_2SiO_3, higher quantities of bound water is found, except for the results at 2 days. Samples prepared with 50% and 75% Na_2SiO_3 show amounts of bound water similar to those of sample prepared with 100% Na_2SiO_3, demonstrating that hydration occurs similarly between these samples, producing similar amounts of hydration products.

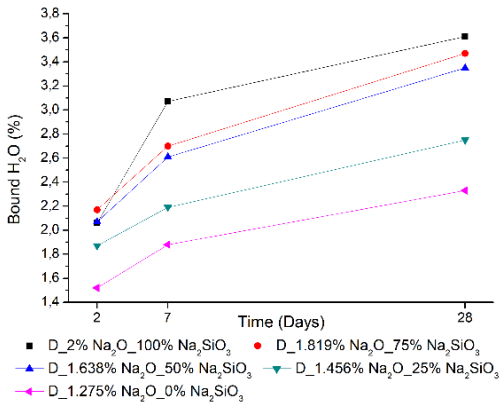

Figure 11 – TGA results for paste samples with different amounts of Na_2SiO_3.

3.4.2. Na_2SO_4 and $CaSO_4$ study

3.4.2.1. Compressive Strength Tests

Figures 12 and 13 display the development of compressive strength over the time of hydration for paste samples prepared with Na_2SO_4 and $CaSO_4$, respectively and for a paste sample prepared with Na_2SiO_3 as a reference.

Every paste samples with Na_2SO_4 revealed lower mechanical performance than paste with Na_2SiO_3 at 7 and 28 days. Within pastes with Na_2SO_4, the paste from binder E developed slightly lower compressive strengths than pastes from binder D and F. The increase in concentration of Na_2SO_4 in the alkaline solution resulted in an unimpressive improvement of the mechanical performance.

Paste sample with $CaSO_4$ show even lower compressive strengths than samples activated with Na_2SO_4. The results of sample *D_1.275%Na_2O_4.39%wt.$CaSO_4$* show that the increase in $CaSO_4$ concentration resulted in a decrease in mechanical performance, except at 28 days, compared with the other sample from binder D, *D_1.275%Na_2O_1.59%wt.$CaSO_4$*.

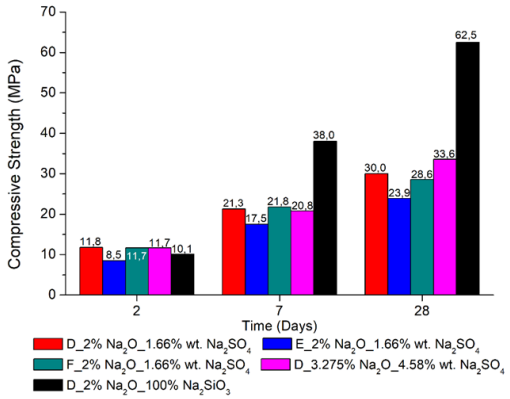

Figure 12 – Compressive strength results for paste samples activated with Na_2SO_4.

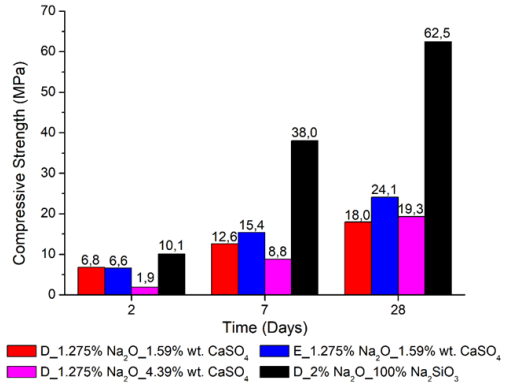

Figure 13 – Compressive strength results for paste samples activated with $CaSO_4$.

3.4.2.2. Thermogravimetric analysis

Figures 14 and 15 show the evolution of the amount of bound water over time of hydration for the paste samples prepared with Na_2SO_4 and $CaSO_4$, respectively, and for a paste sample prepared with Na_2SiO_3 as a reference.

TGA results show that the amount of bound water of paste samples prepared, either with Na_2SO_4 or $CaSO_4$, is lower than those found in paste samples prepared with Na_2SiO_3. All paste samples with Na_2SO_4, except for sample from binder D with lower concentration, present similar amounts of bound water at all ages, which indicates that hydration is developing identically between these samples, producing identical amounts of hydration products. Thus, the increase in Na_2SO_4 concentration did promote the formation of slightly more hydration products. Paste samples prepared with $CaSO_4$ presented even lower amount of bound water than paste sample prepared with Na_2SO_4.

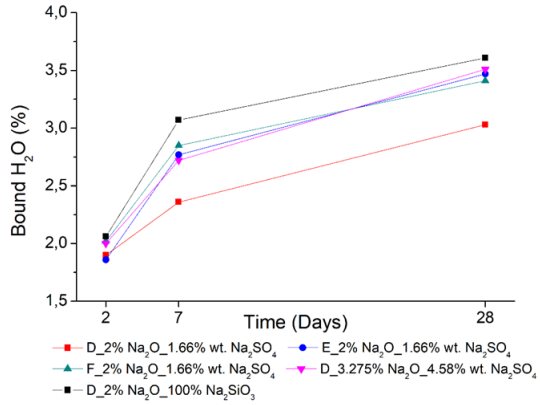

Figure 14 – TGA results for paste samples activated with Na_2SO_4.

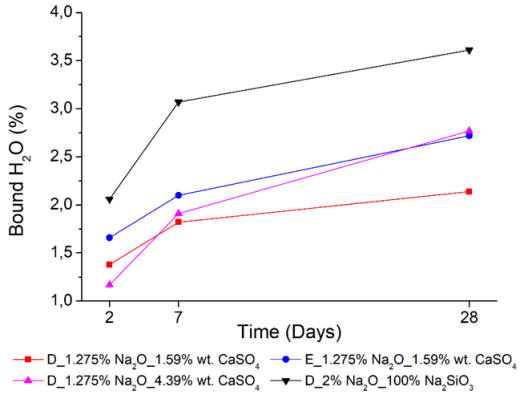

Figure 15 – TGA results for paste samples activated with $CaSO_4$.

3.4.3. W/C ratio optimization study

3.4.3.1. Workability Tests

Table 1 shows the results for the workability tests for mortar with different W/C ratios. As expected, increasing the W/C ratio also increases the workability of the mortar.

Table 1 – Workability results of mortars with different W/C ratios.

A/C	Workability (%)
0,38	61
0,365	47
0,35	28
0,335	18

3.4.3.2. Compressive Strength Tests

Figure 16 displays the development of compressive strength for mortar samples with different W/C ratios showing the best mechanical performance in mortars is achieved for the sample with W/C = 0.365, which reached higher compressive strengths at all ages than the other samples.

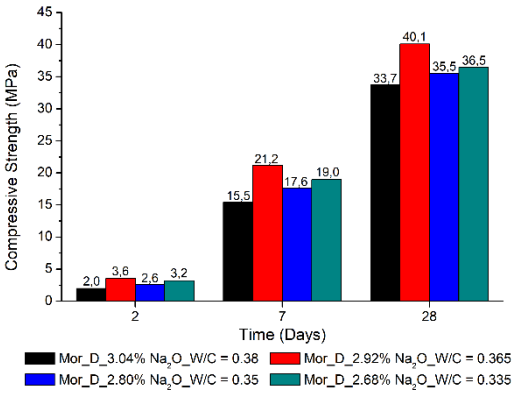

Figure 16 – Compressive strength results for mortar samples with different W/C ratios.

3.4.3.3. Thermogravimetric analysis

Figure 17 shows the bound water development for mortar samples with different W/C ratios. TGA measurements show that higher amounts of bound water were found for sample with W/C = 0.365.

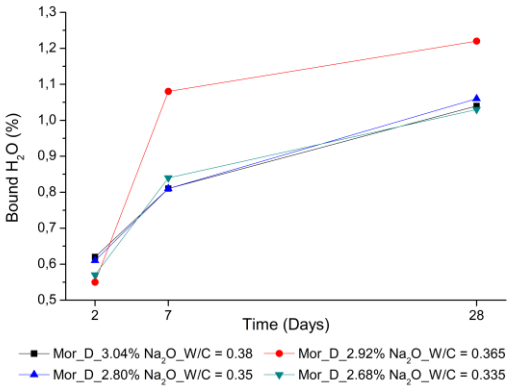

Figure 17 – TGA results for mortar samples with different W/C ratios.

4. Discussion

The calorimetry experiment (Figure 1) showed that sample with higher fineness reached the maximum of the main hydration peak earlier and released a higher amount of heat after 7 days, which is in agreement with the compressive strength tests at 7 days (Figure 2) and TGA results (Figure 3), as the greater amount of bound water is an indicator of greater amount of hydration products formed, namely C–S–H, and consequently, better mechanical performance. This result can be explained by the increase in surface area of the binder with higher fineness, that represents an increase of reaction sites, leading to a higher formation of hydration products at early stages.

The compressive strength tests in the mill study revealed that paste samples with similar fineness ground in different mills have identical mechanical performances, differing 4% at 2 and 7 days, and around 11% at 28 days, for pastes of binder D, Figure 4. Thermogravimetric results confirm the compressive strength results, revealing that samples with similar fineness from different mills presented identical amounts of bound water, diverging at most around 5%, Figure 5. These small differences can be explained from the preparation of the sample and the test variability. Given these results, it is possible to conclude that the type of mill used for the grinding does not have a significant effect on the reactivity.

The isothermal calorimetry experiment conducted in the storage time study revealed that the sample with greater storage time had slower reaction kinetics than the sample without storage time. The delaying of the kinetics can be associated to the carbonation that occurs on the surface of the amorphous after grinding. This carbonated surface makes the dissolution of calcium and silica species more difficult, slowing down the kinetics of reaction at early ages. Even so, after 7 days, both samples released similar amounts of heat, indicating that the amount of hydration products in both samples should be similar, which is verified, not only by the compressive strength results, Figure 7, but also by TGA measurements, Figure 8. Consequently, it can be concluded that a storage time of up to 7 days after grinding does not have a significant effect in the overall reactivity of the binder and the amount of hydration products formed, delaying only the very early age kinetics of hydration.

Figure 9 revealed that the peak of hydration was successively delayed as the amount of Na_2SiO_3 increased, which resulted in a more visible induction period. This induction period appeared due the addition of more Na_2SiO_3, which increased the amount of soluble Si in the paste, causing a very low undersaturation of Si in the reaction medium. Low Si undersaturation limits the main driving for the dissolution of $[SiO_4]^{4-}$ species from the amorphous binder. As C–S–H forms and consumes the available Si given by the activator, the level of undersaturation increases, allowing for the dissolution of $[SiO_4]^{4-}$ species from the binder. Thus, the greater the amount of Na_2SiO_3 in the activation solution, the greater the amount of soluble Si, so the longer it takes to start dissolving Si in the binder, which leads to a longer induction time and a later peak of reaction [15]. Figure 10 showed that samples with at least 50% Na_2SiO_3 reached acceptable strengths for all ages. Within these, it is still possible to see that the sample with 75% Na_2SiO_3 achieved essentially equal mechanical performances to those of sample with 100% Na_2SiO_3. Thus, a reduction of, at least, 25% of the amount of Na_2SiO_3 that was previously used is possible without compromising the mechanical performance of the amorphous, allowing to lower the cost of alkaline activation required for this binder.

Both alkaline activation with Na_2SO_4 (Figure 12) and $CaSO_4$ (Figure 13) show much lower

compressive strengths than alkaline activation with Na_2SiO_3. The best mechanical performances achieved by activations with Na_2SO_4 and $CaSO_4$ roughly equal the performances achieved by an activation with only 25% Na_2SiO_3 of the amount normally used (Figure 10), which defeats the purpose of using these less expensive alternative activators.

Regarding mortars, the results showed that, as W/C ratio increased, so did the workability (Table 1), as expected. Nonetheless, mortar samples prepared with W/C = 0.38 and W/C = 0.365, whose workability values fall below the ones typically reached by traditional OPC with W/C = 0.5, around 83%, showed acceptable workability and a behaviour similar to that of a cement based adhesives. In relation to compressive strength, the better performance is achieved for a W/C = 0.365 (Figure 16), whose values surpass all the other samples, within the tested W/C ratios, at all ages, due to higher amount of C–S–H formed in this sample, as revealed by Figure 17.

5. Conclusions

In this work it was found that fineness presents an important impact in the early age strength development (until 7 days), whereas this effect diminishes for longer hydration ages (from 28 to 90 days). It was also found that the type of mill used to grind the amorphous binder does not have a significant effect on its hydraulic reactivity, nor does a storage time of up to 7 days after grinding.

Furthermore, it was found that a 25% reduction of the amount of Na_2SiO_3 used in previous studies was possible without compromising mechanical performance, reaching similar, or even better, compressive strengths than the usual amount of Na_2SiO_3, allowing for costs reduction in the alkaline activation of this binder. It was also found that neither Na_2SO_4 nor $CaSO_4$ could provide competitive mechanical performances to those developed by alkaline activation with Na_2SiO_3. Finally, it was found that the best mechanical performances in mortars were achieved for a W/C = 0.365. while a W/C = 0.38 showed the best workability.

6. Bibliography

1. IEA, *Cement – Tracking Industry*, 2019. [Accessed on 6/06/2020]; Available from: https://www.iea.org/reports/tracking-industry-2019.
2. Hasanbeigi, A., L. Price, and E. Lin, "Emerging energy-efficiency and CO2 emission-reduction technologies for cement and concrete production: A technical review"*, Renewable and Sustainable Energy Reviews*, vol. 16, no. 8, pp. 6220-6238, 2012.
3. Habert, G., "Assessing the environmental impact of conventional and 'green' cement production", in *Eco-efficient Construction and Building Materials*, F. Pacheco-Torgal, et al., Editors, Woodhead Publishing, 2014, pp. 199-238.
4. Andrew, R.M., "Global CO2 emissions from cement production"*, Earth Syst. Sci. Data*, vol. 10, no. 1, pp. 195-217, 2018.
5. Jean-Louis Cohen, G.M.M., *Liquid Stone : New Architecture in Concrete*, 1st ed, Princeton Architectural Press, 2006.
6. *Cement production worldwide from 1995 to 2019*. [Accessed on 14/03/2020]; Available from: https://www.statista.com/statistics/1087115/global-cement-production-volume/.
7. Taylor, H.F.W., *Cement Chemistry*, 2nd ed, Thomas Telford, 1997.
8. Antoni, M., et al., "Cement substitution by a combination of metakaolin and limestone"*, Cement and Concrete Research*, vol. 42, no. 12, pp. 1579-1589, 2012.
9. Staněk, T. and P. Sulovský, "Active low-energy belite cement", *Cement and Concrete Research*, vol. 68, pp. 203-210, 2015.
10. Provis, J.L. and S.A. Bernal, "Geopolymers and Related Alkali-Activated Materials"*, Annual Review of Materials Research*, vol. 44, no. 1, pp. 299-327, 2014.
11. Santos, R.L., et al., "Novel high-resistance clinkers with 1.10<CaO/SiO2<1.25: production route and preliminary hydration characterization"*, Cement and Concrete Research*, vol. 85, pp. 39-47, 2016.
12. Santos, R.L., et al., "Alkali activation of a novel calcium-silicate hydraulic binder with CaO/SiO2 = 1.1"*, Journal of the American Ceramic Society*, vol. 101, no. 9, pp. 4158-4170, 2018.
13. IPQ, *EN196-1 - Métodos de ensaio de cimentos. Parte 1: Determinação das resistências mecânicas*, 2017.
14. CEN, *Methods of test for mortar for masonry - Part 3: Determination of consistence of fresh mortar (by flow table)*, 1999.
15. Zuo, Y. and G. Ye, "Preliminary Interpretation of the Induction Period in Hydration of Sodium Hydroxide/Silicate Activated Slag"*, Materials*, vol. 13, no. 21, pp. 4796, 2020.

7. Annexes

Table 2 – Chemical composition of raw materials and produced amorphous hydraulic binders.

		Composition (wt.%)								
Raw materials	**% wt.**	**SiO_2**	**Al_2O_3**	**F_2O_3**	**CaO**	**MgO**	**K_2O**	**Na_2O**	**TiO_2**	**Others**
Limestone	≈ 50%	0,85	0,22	0,29	55,21	0,2	0,02	0,05	0,02	0,06
Sand	≈ 30%	96,95	1,29	0,17	0,07	0	0,53	0,1	0,04	0,01
Cement raw meal	≈ 20%	13,19	3,36	2,03	43,69	0,76	0,64	0,09	0,18	0,34
Amorphous	**C/S**									
A	1,006	49,63	2,32	0,73	46,58	0,35	0,34	0,11	0,09	0,1
B	1,059	48,33	1,99	0,51	47,75	0,32	0,24	0,14	0,09	0,15
C	1,022	47,97	3,58	0,96	45,76	0,32	0,35	0,2	0,1	0,05
D	1,046	47,64	3,34	1,02	46,49	0,31	0,36	0,15	0,1	0,07
E	1,044	48,55	2,15	0,72	47,29	0,31	0,32	0,13	0,09	0,11
F	1,038	47,88	3,15	0,96	46,38	0,31	0,31	0,14	0,1	0,13

Table 3 – Milling/alkali-activation conditions and adopted nomenclature for each sample in each study.

Type	**Binder**	**Mill**	**Milling time (min)**	**Storage time (days)**	**Sample name**
			Fineness study		
Pastes	D	Ring	1	<1	D_1min_Ring
		Ring	220	<1	D_3min_Ring
			Mill study		
Pastes	B	Ring	1	<1	B_1min_Ring
		Ring	3	<1	B_3min_Ring
			Storage time study		
Pastes	A	Ring	3	<1	A_3min_Ring_1dayST
		Ball	3	7	A_3min_Ring_7daysST

			Na_2SiO_3 reduction			
Type	**Binder**	**% Na_2O**	**Activators**	**W/C**	**% Na_2SiO_3**	**Sample name**
Pastes	D	2	NaOH + Na_2SiO_3	0.25	100	D_2%Na_2O_100%Na_2SiO_3
		1.819		0.25	75	D_1.819%Na_2O_75%Na_2SiO_3
		1.638		0.25	50	D_1.638%Na_2O_50%Na_2SiO_3
		1.456		0.25	25	D_1.456%Na_2O_25%Na_2SiO_3
		1.275		0.25	0	D_1.275%Na_2O_0%Na_2SiO_3
			Na_2SO_4 and $CaSO_4$ study			
Type	**Binder**	**% Na_2O**	**Activators**	**W/C**	**%wt. activator**	**Sample name**
Pastes	D	2	NaOH + Na_2SO_4	0.25	1.66	D_2%Na_2O_1.66%wt. Na_2SO_4
	E	2		0.263	1.66	E_2%Na_2O_1.66%wt. Na_2SO_4
	F	2		0.27	1.66	F_2%Na_2O_1.66%wt. Na_2SO_4
	D	3.275		0.25	4.58	D_3.275%Na_2O_4.58%wt. Na_2SO_4
	D	1.275	NaOH + $CaSO_4$	0.25	1.59	D_1.275%Na_2O_1.59%wt. $CaSO_4$
	E	1.275		0.27	1.59	E_1.275%Na_2O_1.59%wt. $CaSO_4$
	D	1.275		0.25	4.39	D_1.275%Na_2O_4.39%wt. $CaSO_4$
			W/C ratio optimization study			
Type	**Binder**	**% Na_2O**	**Activators**	**W/C**		**Sample name**
Mortars	D	3.04	NaOH + Na_2SiO_3	0.38		Mor_D_3.04%Na_2O_W/C = 0.38
		2.92		0.365		Mor_D_2.92%Na_2O_W/C = 0.365
		2.80		0.35		Mor_D_2.80%Na_2O_W/C = 0.35
		2.68		0.335		Mor_D_2.68%Na_2O_W/C = 0.335